

Storage Is Not Memory: A Retrieval-Centered Architecture for Agent Recall

Joshua Adler Guy Zehavi

Sauron Labs

josh@sauronlabs.ai

Abstract

Extraction at ingestion is the wrong primitive for agent memory: content discarded before the query is known cannot be recovered at retrieval time. We propose **True Memory**, a six-layer architecture that shifts the center of the system from a storage schema to a multi-stage retrieval pipeline operating over events preserved verbatim. The full system runs as a single SQLite file on commodity CPU with no external database, vector index, graph store, or GPU. On LoCoMo (Maharana et al., 2024), 1,540 questions across 10 multi-session conversations, True Memory Pro reaches 93.0% accuracy (3-run mean, semantic-match judge; rankings are valid across systems but absolute scores exceed published strict-match baselines) against 61.4% for Mem0, 65.4% for Supermemory, and approximately 71% for Zep (Rasmussen et al., 2025) under a matched gpt-4.1-mini answer model, and 94.5% for EverMemOS, which uses a GPU-served embedder and a Neo4j graph store. On LongMemEval (Wu et al., 2025), 500 questions across multi-session conversations, True Memory Pro reaches 87.8% (3-run mean). On BEAM-1M (Tavakoli et al., 2026), 700 questions across 35 conversations at the 1-million-token scale, True Memory Pro reaches 76.6% (3-run mean), above the prior published result of 73.9% for Hindsight (Latimer et al., 2025). A 56-configuration ablation shows a 1.3-percentage-point spread within the top-performing configuration family. The system also includes an encoding gate (novelty, salience, prediction error) that filters ingestion in production; it is disabled in all reported benchmark numbers because current evaluation instruments reward total recall and cannot score selective ingestion. Gate evaluation is deferred to future work.

1 Introduction

Agent memory has emerged as a commercial product category for language models operating

across sessions, days, or months, including Mem0 (Chhikara et al., 2025), Zep (Rasmussen et al., 2025), Graphiti (Zep AI, 2024), Supermemory (Supermemory, 2024), and EverMemOS (Hu et al., 2026). These systems share a structural pattern in which, at ingestion, a language model parses incoming conversational content into a structured representation, whether atomic facts (Chhikara et al., 2025), entity nodes in a knowledge graph (Rasmussen et al., 2025; Zep AI, 2024), hierarchical summaries (Supermemory, 2024), or graph-plus-embedding hybrids (Hu et al., 2026), that is then stored in a vector database or graph store and retrieved by similarity at query time.

This pattern inherits the wrong primitive from document search infrastructure, which uses approximate nearest-neighbor indexing (Malkov and Yashunin, 2018) as exposed by managed or open-source products such as Pinecone, Chroma, Weaviate, and Qdrant (Pinecone et al., 2026), where structured records are extracted at ingestion, indexed, and retrieved by similarity. Because extraction runs before the query is known, content discarded at ingestion cannot be recovered at retrieval time.

Retrieval-augmented generation (Lewis et al., 2020) and a body of subsequent work partially mitigate these limitations through query expansion via hypothetical document embeddings (Gao et al., 2023), cross-encoder reranking over initial candidates (Nogueira and Cho, 2019), and reciprocal rank fusion of lexical and semantic signals (Cormack et al., 2009). These refinements improve recall over plain similarity search, but they operate on the structured representation produced at ingest and therefore inherit whatever that step preserved.

We present **True Memory**, an agent memory architecture that applies an encoding gate at ingestion rather than extracting incoming conversational events into structured records. The gate scores

Technical report. Sauron Labs, 2026.

each event for novelty, salience, and prediction error, and events that exceed threshold are preserved verbatim, while higher-order structure such as summaries, entity profiles, and consolidation is computed post-ingestion or deferred to query time. Grounded in reconstructive recall (Bartlett, 1932), the episodic/semantic distinction (Tulving, 1972), and levels-of-processing effects on retrievability (Craik and Lockhart, 1972), with the taxonomy of memory distortions from Schacter (2001) informing our treatment of contradictions, True Memory is implemented as a single SQLite file running on edge compute.

The contributions of this paper are fourfold:

1. **Architectural reframing.** We formalize agent memory as a retrieval architecture rather than a storage schema (Figure 1), with encoding, consolidation, and query-time ranking as cooperating stages of the same pipeline rather than independent modules separated by a database.
2. **Encoding gate.** We introduce a three-signal gated ingestion mechanism (novelty, salience, prediction error) whose novelty and prediction-error signals query the same stored message substrate that the retrieval layers use, while salience scores the incoming event in isolation; ingestion and retrieval therefore share a common representation rather than being separated by a schema boundary.
3. **Empirical evidence.** We report 93.0% on LoCoMo (1,540 questions, 3-run mean), 87.8% on LongMemEval (500 questions, 3-run mean), and 76.6% on BEAM-1M (700 questions at the 1-million-token scale, 3-run mean) under gpt-4.1-mini, trailing only EverMemOS on LoCoMo and exceeding all prior published results on BEAM-1M, with a 56-configuration ablation showing a 1.3-percentage-point spread within the top-performing subfamily.
4. **Retrieval-as-bottleneck diagnostic.** On 357 LoCoMo questions answered incorrectly by an early True Memory iteration, supplying the full conversation to the same answer model recovered 92%, locating the bottleneck in the retrieval pipeline rather than the storage layer.

2 Background

Vector database infrastructure built on HNSW-class indexing (Malkov and Yashunin, 2018), as exposed by products including Pinecone, Chroma, Weaviate, and Qdrant (Pinecone et al., 2026), was designed for large-scale document search, where a document is chunked once at indexing time, embedded into a dense vector space, and served by approximate nearest-neighbor lookup. The design is defensible where the corpus is stable, queries fall within a predictable range, and stored items carry roughly equivalent informational weight, since under those conditions the chunk boundaries and the fixed representation are unlikely to matter for most future queries.

Retrieval-augmented generation (Lewis et al., 2020) adapted this infrastructure to language models, and commercial agent memory systems (Chhikara et al., 2025; Hu et al., 2026; Rasmussen et al., 2025; Supermemory, 2024; Zep AI, 2024) extended it to multi-session conversational settings. Query-time refinements accumulated on top, including query expansion via hypothetical document embeddings (Gao et al., 2023), cross-encoder reranking over initial candidates (Nogueira and Cho, 2019), and reciprocal rank fusion of lexical and semantic signals (Cormack et al., 2009); each refinement raises recall over what was preserved, but none of them change what gets preserved.

None of the conditions that justified the document-search design hold in agent memory: the corpus grows with every conversational turn, queries arrive days or weeks after content was stored and frequently ask about details the extractor had no reason to preserve, and informational weight is highly non-uniform, with details mentioned once in passing sometimes serving as the key to a question asked months later.

A parallel line of ML research modifies how language models handle information internally. Memory networks introduce memory slots inside the model’s forward pass (Sukhbaatar et al., 2015), and MemGPT pages content in and out of the model’s context window at runtime (Packer et al., 2023). These systems change how a model processes the information it already has, whereas True Memory addresses the prior question of which information reaches the model in the first place. To our knowledge, True Memory is among the first publicly-described agent memory architectures that treat gated ingestion and query-time relevance judgment

as cooperating mechanisms, with two of three gate signals querying the same stored message substrate that serves retrieval. The framing draws on reconstructive memory as described by [Bartlett \(1932\)](#), the episodic/semantic distinction due to [Tulving \(1972\)](#), and the complementary-learning-systems account of [McClelland et al. \(1995\)](#).

Concurrent with this work, several groups have independently explored retrieval-centered architectures for agent memory. These systems share the premise that verbatim event preservation outperforms extraction-based ingestion; they differ in retrieval-pipeline design, storage substrate, and deployment model. In a related direction, [Li et al. \(2026\)](#) propose a query-focused and memory-aware reranker for long-context processing, extending cross-encoder reranking with explicit memory conditioning; their work is complementary to the multi-stage pipeline described here. True Memory’s distinguishing characteristic is the single-SQLite-file implementation with zero external dependencies, the three-signal encoding gate, and the emphasis on commodity-hardware deployment.

3 Design Principles

A database returns what was written, whereas a memory returns what is reconstructed at the moment of recall, a distinction foundational in cognitive neuroscience ([Bartlett, 1932](#); [Schacter, 2001](#)). Extraction-based agent memory inverts this relationship, committing content to a fixed schema at ingestion and treating retrieval as lookup over that schema, so that the representation becomes the memory. When a query arrives that the schema did not anticipate, the representation cannot accommodate it, and the memory is not available to be retrieved regardless of what was originally said.

A memory system is therefore defined by what it does at the moment of recall rather than by what it wrote down earlier. [Tulving \(1972\)](#)’s distinction between episodic and semantic memory is framed at retrieval, where the same underlying substrate serves both and what surfaces depends on how the cue interrogates it, and [Craik and Lockhart \(1972\)](#) showed that depth of encoding determines later retrievability, coupling encoding and retrieval across time rather than separating them into independent stages.

The scaling argument follows from the same re-

framing. Language models have finite context windows while conversations extend without bound, so retrieval is the mechanism that lets the bounded window carry the unbounded history. The brain solves the analogous problem through consolidation, by which memories are reorganized over time with emotionally or consequentially salient content preferentially preserved ([Cahill and McGaugh, 1995](#); [Squire and Alvarez, 1995](#)); consolidation on this view is not compression for storage efficiency but preparation for retrieval under cues that cannot be anticipated at encoding. Neither dumping the entire conversation into context nor extracting a lossy summary at ingestion scales to unbounded histories, whereas selective preservation and selective surfacing, decided separately and at different moments, supplies the scalable path.

4 Architecture

True Memory is organized into six layers (L0–L5) that operate across three time-separated phases: *ingestion*, *post-ingestion batch processing*, and *query-time retrieval*. Stored events are retained in the form they arrived in, and interpretive structure is computed later. The ten pipeline stages below specify each layer by its typed input and output. We adopt the convention, following information-retrieval literature ([Cormack et al., 2009](#)), that d denotes a candidate item and q denotes a user query; throughout §4, d specifically refers to a candidate event, a single admitted message row in the L1 messages table, rather than a document in the traditional document-retrieval sense.

4.1 Pipeline stages

The ten pipeline stages below reference the six layers (L0–L5) as follows: Stage 1 uses all three gate signals (L0/L3/L5 derived), Stage 2 = L1 writer, Stage 3 = L4 consolidator, Stage 4 = L5 predictive coder, Stage 5 = L0 engram updater, Stage 6 = L1 lexical retrieval, Stage 7 = L2 dense retrieval, Stage 8 = RRF fusion (cross-layer), Stage 9 = L3 salience reweighter, Stage 10 = cross-encoder reranker.

Ingestion phase

Stage 1: Encoding Gate. Input: raw event e_t with text and metadata (sender, timestamp, modality). Output: binary admit decision plus a signal tag set $\{n_t, s_t, \pi_t\}$ written to the event’s metadata on admit.

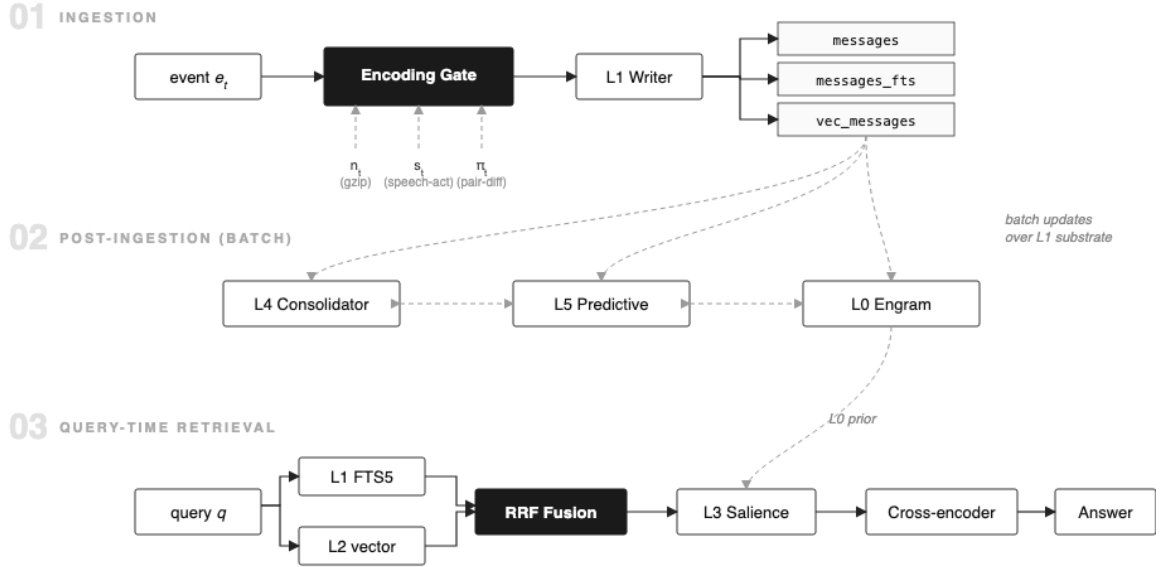


Figure 1: True Memory’s six-layer architecture across three time-separated phases. **Ingestion (01):** the encoding gate admits or rejects each event e_t based on novelty (n_t), salience (s_t), and prediction error (π_t), computed through independent signal mechanisms; novelty and prediction error query the stored message substrate, while salience scores the event in isolation. Admitted events are written verbatim to `messages` with corresponding updates to the FTS5 lexical and sqlite-vec dense indices. **Post-ingestion (02):** batch processes read the L1 event substrate to update L4 consolidation artifacts, the L5 surprise index, and the L0 personality engram. **Query-time (03):** L1 lexical and L2 dense candidates are fused via reciprocal rank fusion, reweighted by L3 saliency conditional on the L0 speaker engram (dashed *prior* arrow), and reranked by a cross-encoder before the top- k are passed to the answer model.

Novelty and salience operate on different axes. Novelty is computed against the stored neighborhood returned by L2 and scores the event relative to what the substrate already contains; salience is computed over the event in isolation and scores properties of the event itself: category, affect, information density. A restatement of a known preference therefore has low novelty but high salience, and a novel passing detail has high novelty but low salience; the gate combines both rather than substituting one for the other.

For each incoming event e_t , the gate computes three signals, each through its own mechanism. Novelty and prediction error query the stored message substrate; salience scores the event in isolation:

- *Novelty* (n_t) measures how much new information e_t adds to stored memories using gzip compression cost. The gate retrieves the nearest stored messages, concatenates them into a memory text M , and computes

$$n_t = \frac{|\text{gz}(M \parallel e_t)| - |\text{gz}(M)|}{|\text{gz}(e_t)|},$$

where $\text{gz}(\cdot)$ denotes gzip compression at level 6 and \parallel denotes byte concatenation. Redundant information compresses cheaply against the memory context, yielding low n_t ; novel information is incompressible, yielding high n_t . The signal returns 1.0 when memory is empty and 0.05 for trivially short messages (compressed size below 10 bytes). This replaced cosine-similarity inversion, which is anti-correlated with novelty in conversational data: noise like “ok” is semantically distant from factual memories while important updates are semantically close. Validated

in a 120-variant sweep: AUC 0.788 vs. 0.484 for cosine baseline. Implementation: `truememory.ingest.encoding_gate`.

- *Saliency* (s_t) delegates to a hybrid scorer (`truememory.ingest.encoding_saliency`) that routes on message length: messages of 50 characters or fewer are scored by a rule-based speech-act classifier that is length-independent, returning fixed scores by linguistic function (e.g., commitments \rightarrow 0.8, corrections \rightarrow 0.6, noise \rightarrow 0.02, questions \rightarrow 0.2); messages longer than 50 characters are scored by the L3 retrieval saliency scorer (`truememory.saliency.compute_message_saliency`), which evaluates length, numbers, dates, and emotional markers.
- *Prediction error* (π_t) uses embedding pair-difference scoring. The gate embeds the cross-pair (e_t [SEP] m_1) and the self-pair (m_1 [SEP] m_1), where m_1 is the nearest stored memory, using the same embedding model that serves vector search. Prediction error is

$$\pi_t = 1 - \cos(\mathbf{v}_{\text{cross}}, \mathbf{v}_{\text{self}}).$$

When the cross-pair embedding diverges from the self-pair, the message says something different about the same topic. The signal applies two early-exit filters: messages classified as noise by the saliency scorer are assigned $\pi_t = 0$ without embedding, and messages whose nearest stored memory has low topical relevance (below a cosine threshold) are also assigned $\pi_t = 0$. Validated in a 200-variant sweep: AUC 0.730 standalone, gate AUC 0.816 in three-signal combination; independent of novelty ($r = 0.30$) and saliency ($r = 0.23$). No additional model is required. Implementation: `truememory.ingest.encoding_gate`.

The gate applies a saliency floor $s_{\min} = 0.10$: messages whose saliency falls below s_{\min} are rejected regardless of their gate score, preventing high-novelty off-topic noise from passing. For messages above the floor, admit e_t iff

$$\frac{\lambda_n \cdot n_t + \lambda_s \cdot s_t + \lambda_\pi \cdot \pi_t}{\lambda_n + \lambda_s + \lambda_\pi} \geq \tau + \Delta_c, \quad (1)$$

where Δ_c is a per-category threshold offset (correction -0.06 , decision -0.04 , relationship -0.04 , all others 0) that lowers the bar for high-value categories. The weights $(\lambda_n, \lambda_s, \lambda_\pi, \tau) = (0.25, 0.20, 0.30, 0.30)$ are production defaults. The numerator is normalized by the weight sum so the score lands in $[0, 1]$ regardless of weight magnitudes.

In the benchmark configuration used throughout §6, the gate is disabled and every input event is admitted ($\tau = -\infty$).

Stage 2: L1 Writer. Input: admitted event plus metadata and signal tag set. Output: one row in `messages`, a corresponding update to the `messages_fts` FTS5 index, and a 256-dimensional vector row in `vec_messages` (sqlite-vec).

Post-ingestion phase (batch)

Stage 3: L4 Consolidator.¹ Input: event clusters over a sliding window of recent messages rows. Output: summary rows (one per cluster), contradiction records (pairs of rows whose claims conflict, indexed by entity and predicate), and timeline rows (time-ordered assertions with superseded-by links).

Stage 4: L5 Predictive Coder.² Input: the event stream in temporal order. Output: a per-event surprise score $\sigma_t \in [0, 1]$ stored in `surprise_scores` and used as a retrieval boost. In the production implementation, σ_t is a weighted combination of the fraction of newly-extracted fact fingerprints (numbers, proper nouns, dates, event keywords, definitional predicates) not yet present in the accumulated fact set, plus small length, detail, and event bonuses, with explicit contradiction detection for update verbs. There is no learned predictor \hat{v}_t in the current implementation; the surprise signal is computed directly over extracted fact sets rather than as an L2 residual.

Stage 5: L0 Engram Updater.³ Input: full event history for a given speaker. Out-

¹Inspired by memory consolidation as described in [Squire and Alvarez \(1995\)](#).

²Inspired by the predictive-coding framework of [Rao and Ballard \(1999\)](#).

³Inspired by the theory-of-mind framework of [Gallagher and Frith \(2003\)](#).

put: a speaker-preference attribute map in `entity_profiles` (one row per distinct entity), plus a 256-dimensional character-n-gram style vector in `entity_style_vectors` (hashed char-(3,4,5)-grams, L2-normalized, mean-pooled across a speaker’s messages), both refreshed on schedule. At query time the style vector is used as a retrieval prior, scoring candidate messages by cosine similarity to the queried entity’s writing profile.

Query-time phase

Stage 6: L1 Lexical Retrieval. Input: query q . Output: candidate set $C_1 = \text{top-}k$ FTS5 matches over `messages_fts` (rank by BM25).

Stage 7: L2 Dense Retrieval. Input: query q , embedded to v_q . Output: candidate set $C_2 = \text{top-}k$ cosine-nearest rows from `vec_messages`.

Stage 8: RRF Fusion. Input: (C_1, C_2) (and the optional separation list). Output: fused candidate set C_{fused} ranked by a per-source-weighted extension of reciprocal rank fusion. The original formulation of Cormack et al. (2009) aggregates candidate rankings as

$$\text{RRF}_{\text{Cormack}}(d) = \sum_{r \in R} \frac{1}{k + r(d)}, \quad k = 60, \quad (2)$$

where R is the set of contributing rank lists, $r(d)$ is the rank of d in list r , and $k = 60$ is the smoothing constant from that work; individual rank lists are not weighted, so the formulation is the uniform case $w_r \equiv 1$. True Memory extends this with a per-source weight w_r to reflect the empirically different contributions of lexical and dense rank lists in multi-session conversational retrieval, and to accommodate the optional separation rank list whose signal is weaker than either primary source:

$$\text{RRF}(d) = \sum_{r \in R} w_r \cdot \frac{1}{k + r(d)}, \quad k = 60, \quad (3)$$

where R contains the FTS5, dense, and (when present) separation rank lists, with $w_{\text{fts}} = w_{\text{vec}} = 1$ and $w_{\text{sep}} = 0.8 \times w_{\text{vec}}$ in the reference implementation; separation search fires only when the corpus contains more than five distinct senders, because in two- or three-person conversations the sender/recipient prefix produces a

uniform ranking that dilutes the primary signals (`truememory/hybrid.py`). The smoothing constant $k = 60$ is unchanged from Cormack et al. (2009). A principled calibration sweep over the source weights is left for future work.

Stage 9: L3 Saliency Reweigher.⁴ Input: C_{fused} , plus query-side signals (question type, timestamp) and the L0 speaker engram. Output: C_{fused} reweighted by a pipeline of conditional scalar adjustments applied sequentially to each candidate’s RRF score:

$$\text{score}_{L_3}(d, q) = \text{RRF}(d) \circ f_t(d, q) \circ f_{L_0}(d), \quad (4)$$

where \circ denotes sequential application (i.e., each factor either multiplies the running score or injects new candidates) and each factor fires only when its triggering condition is met:

- $f_t(d, q)$ is a conditional temporal boost: when the query carries temporal intent and the candidate d already appears in the temporally-filtered result set, the running score is multiplied by 1.3; otherwise $f_t = 1$ (`truememory/engine.py`).
- $f_{L_0}(d)$ is a conditional personality-prior injection: when the query has personality intent, L0 profile and style-vector results are appended to the candidate set with scores scaled to $0.8 \times \max(\text{existing scores})$ for entity-profile results and $0.9 \times \max$ for style-vector results, so that the L0 prior informs but does not dominate factual retrieval (`truememory/engine.py`).

Results falling below a minimum saliency threshold are dropped from the candidate set before reranking. When the `surprise_scores` table is populated, candidates with a positive surprise score $\sigma_t > 0$ have their score multiplied by $(1 + \alpha \cdot \sigma_t)$ where $\alpha = 0.2$ (configurable via `TRUEMEMORY_ALPHA_SURPRISE`); candidates with $\sigma_t = 0$ are left untouched, and the step is a no-op when the surprise index has not been built. Each multiplicative factor is scalar, so $\text{score}_{L_3}(d, q)$ is itself scalar. The pipeline is compositional: factors fire independently and in sequence, with inactive factors contributing 1 (identity).

⁴Inspired by levels-of-processing effects on retrievability (Craik and Lockhart, 1972).

Stage 10: Cross-encoder Reranker with Modality Fusion. Input: $(q, d.text)$ pairs for the top N items in the reweighted C_{fused} . Output: scalar relevance score per pair, optionally adjusted by a modality factor $f_m(d, q)$ that examines the candidate’s modality and the question type of the query (detail questions penalize summary modalities by 0.7×; synthesis questions boost them by 1.2×; general questions apply no adjustment), implemented in `truememory/reranker.py`. The top- k (default $k = 10$) after sorting are passed to the answer model. In the benchmark configuration used throughout §6, the pre-rerank window is 100 (see Table 1).

5 Implementation

True Memory’s entire persistent state is a single SQLite database file, and its runtime dependencies are Python and standard scientific-computing libraries. No external database, vector index, graph store, GPU, or cloud service is required at any configuration.

Storage substrate. The full storage layer consists of SQLite with the FTS5 full-text-search module (Hipp and contributors, 2000) for lexical search and `sqlite-vec` (Garcia, 2024) for dense-vector retrieval. Events are stored verbatim in a `messages` table with metadata (sender, recipient, timestamp, category, modality), while entity profiles, summaries, fact timelines, and surprise indices occupy their own tables populated by post-ingestion batch processes. The database file is portable, backupable as a single file, and inspectable with any SQLite tool.

5.1 Schema snippet

The following is a verbatim excerpt of the production DDL from `truememory/storage.py` (Figure 2); tables and triggers not central to the exposition are elided.

```

L1 EVENT SUBSTRATE
-- Verbatim messages with metadata.
CREATE TABLE IF NOT EXISTS messages (
  id          INTEGER PRIMARY KEY AUTOINCREMENT,
  content     TEXT NOT NULL,
  sender     TEXT DEFAULT '',
  recipient  TEXT DEFAULT '',
  timestamp  TEXT DEFAULT '',
  category   TEXT DEFAULT '',
  modality   TEXT DEFAULT '',
  episode_id INTEGER DEFAULT NULL,
  emotional_valence REAL DEFAULT 0.0,
  embedding_separation BLOB DEFAULT NULL
);

L1 LEXICAL INDEX (STAGE 6)
-- Contentless FTS5, synced by triggers.
CREATE VIRTUAL TABLE IF NOT EXISTS messages_fts
USING fts5(content, sender, recipient, category, modality,
           content_rowid='id', tokenize='porter unicode61');

L2 DENSE VECTOR INDEX (STAGE 7)
CREATE VIRTUAL TABLE IF NOT EXISTS vec_messages USING vec0(embedding float[256]);

L0 SPEAKER PRIOR (STAGE 5)
CREATE TABLE IF NOT EXISTS entity_profiles (
  entity      TEXT PRIMARY KEY,
  message_count INTEGER DEFAULT 0,
  tcreate     TEXT DEFAULT '{}',
  communication_style TEXT DEFAULT '{}',
  topics      TEXT DEFAULT '{}',
  relationships TEXT DEFAULT '{}',
  updated_at  TEXT
);

L5 SURPRISE INDEX (STAGE 4)
-- Populated by build_surprise_index().
CREATE TABLE IF NOT EXISTS surprise_scores (
  message_id  INTEGER PRIMARY KEY,
  surprise    REAL NOT NULL DEFAULT 0.0,
  fact_count  INTEGER NOT NULL DEFAULT 0,
  new_fact_count INTEGER NOT NULL DEFAULT 0,
  FOREIGN KEY (message_id) REFERENCES messages(id)
);

```

Figure 2: Production schema excerpt. Each section corresponds to a layer in the architecture of §4: `messages` is the L1 verbatim event substrate, `messages_fts` is the L1 FTS5 lexical index, `vec_messages` is the L2 dense vector index (created lazily by `vector_search.py`), `entity_profiles` is the L0 speaker engram, `entity_style_vectors` stores L0 char-n-gram style profiles, and `surprise_scores` is the L5 prediction-error index (created lazily by `predictive.py`). The full DDL also includes metadata (embedder identity and schema version), `episodes` (6-hour-gap session boundaries), `landmark_events` (life events such as job changes and moves), `causal_edges` (forward/backward cause chains), and `entity_relationships` (Dunbar-hierarchy relationship graph; populated when entity-sheet mode is enabled).

Hardware footprint. A lightweight configuration uses on the order of 30 million total parameters across the embedder and reranker, yielding approximately 123 MB of static model weights at fp32 (approximately 61 MB at fp16), with runtime working-set RAM under 1 GB that is dominated by the Python scientific-computing stack rather than the models themselves; the system runs comfortably on any commodity single-board computer with at least 1 GB of available RAM, and a Raspberry Pi 4 is sufficient for full deployment. Larger configurations use embedders in the hundreds of millions of parameters and approximately

2 to 4 GB of runtime RAM, and none require a GPU. Smaller configurations trade a few points of accuracy for significantly smaller footprint.

Cost profile. True Memory’s infrastructure cost is bounded by local compute, so only the answer-model API call incurs marginal expense; at 100 queries per day this is approximately \$12 per month under `gpt-4.1-mini` pricing. For reference, EverMemOS is open source and free to self-host, though its pipeline requires a Neo4j graph store, a GPU-served embedder, and multi-service cloud orchestration that carry infrastructure costs not reflected in the benchmark harness. Meanwhile, Mem0, Supermemory, and Zep operate on tier-based pricing models in the \$15 to \$400 per month range depending on tier and usage.

5.2 Compute and latency budget

The three tiers use the following model configurations. Embedder: `Model2Vec-potion-base-8M` (Tulkens and van Dongen, 2024) (256-dimensional static embedding) for Edge, and `Qwen3-Embedding-0.6B` (Qwen Team, 2025) truncated to 256 dimensions via Matryoshka representation learning for Base and Pro. Reranker: `cross-encoder/ms-marco-MiniLM-L-6-v2` (22M parameters, CPU-friendly) for Edge, and `Alibaba-NLP/gte-reranker-modernbert-base` (149M parameters) for Base and Pro. Pro adds hypothetical-document query expansion (Gao et al., 2023). Answer model: `openai/gpt-4.1-mini` via the OpenAI API across all tiers. A per-stage latency breakdown is left for future work.

6 Results

The numbers that follow reflect the retrieval stack alone; the encoding-gate disclaimer from the abstract applies throughout. All TrueMemory results were produced on the v0.6.0 pipeline (main branch). OpenRouter API calls were made between April–May 2026.

We evaluate True Memory on three public benchmarks of long-term conversational memory: LoCoMo (Maharana et al., 2024), LongMemEval (Wu et al., 2025), and BEAM-1M (Tavakoli et al., 2026).

Evaluation harness. All three benchmarks are run through the same harness conventions, including deterministic answer and judge generation, `gpt-4o-mini` as a three-run majority judge, and a capped top- k retrieval window feeding the answer model. All True Memory scores in this section are 3-run means unless otherwise noted; individual run scores and standard deviations are reported where the spread is informative.

Answer models for competitor rows are reported per row in Table 2 and vary across systems.

6.1 LoCoMo

Paired comparisons among the three True Memory configurations. On v0.6.0, the 3-run mean gaps are: TM Pro vs. TM Base, 1.0 pp; TM Base vs. TM Edge, 2.4 pp; TM Pro vs. TM Edge, 3.4 pp. The Pro–Base gap is small and may not be statistically resolved; the Base–Edge gap is consistent across all three runs. All three tiers cluster at the origin of the cost-accuracy Pareto frontier (Figure 3a).

Oracle ceiling. The theoretical upper bound on LoCoMo is to supply the full conversation directly to the answer model, bypassing any memory system. Under `gpt-4.1-mini`, this full-context oracle reaches 92.99% (1,432 of 1,540, 95% CI [91.60, 94.16]) at a cost of 45.6 million input tokens per run, or \$0.0129 per correct answer, so True Memory Pro at 93.0% reaches 99.9% of oracle accuracy (Figure 3b) (unrounded: 92.96% 3-run mean vs. 92.99% oracle; both round to 93.0%) at one-fifth the cost per correct. Under Claude Opus 4.6, the same full-context oracle reaches 96.75% (1,490 of 1,540, CI [95.75, 97.53]), indicating that the architectural gain stacks with model gains rather than substituting for them. For reference, `gpt-4.1-mini` with no conversation context at all scores 3.90% (60 of 1,540), which establishes the floor.

6.2 Diagnostic: retrieval is the bottleneck

On an early iteration of True Memory, 357 LoCoMo questions were answered incorrectly. When the answer model was given the full conversation in place of retrieval results on those same 357 questions, 330 of 357 (92.44%, 95% Wilson CI [89.22, 94.75]) were then answered correctly. The

Table 1: Evaluation harness settings.

Setting	LoCoMo	LongMemEval	BEAM-1M
Questions (N)	1,540	500	700
Session structure	10 multi-sess. convs	38–62 haystack sess.	35 convs at 1M tok.
Answer model (TM rows)	<code>gpt-4.1-mini</code>	<code>gpt-4.1-mini</code>	<code>gpt-4.1-mini</code>
Judge model	<code>gpt-4o-mini</code>	<code>gpt-4o-mini</code>	<code>gpt-4o-mini</code>
Judge runs / question	3 (majority)	3 (majority)	3 (majority)
Answer temperature	0	0	0
Judge temperature	0	0	0
Max answer tokens	200	200	200
Retrieval top- k (pre-rerank)	100	100	100

Table 2: LoCoMo accuracy (v0.6.0, 3-run means for True Memory rows) with 95% Wilson confidence intervals. $N = 1,540$.

System	Accuracy	95% CI	Correct	Cost / correct	vs row above
EverMemOS* (Hu et al., 2026)	94.48%	[93.23, 95.51]	1,455	\$0.0010 [†]	—
TM Pro [‡]	93.0%	[91.60, 94.16]	1,432	\$0.0013	$\chi^2 = 4.09, p=0.043$
TM Base [‡]	92.01%	[90.54, 93.26]	1,417	\$0.0011	$\chi^2 = 1.12, p=0.29$
TM Edge [‡]	89.65%	[88.05, 91.07]	1,381	\$0.0010	$\chi^2 = 6.54, p=0.011$
RAG (ChromaDB)	86.17%	[84.35, 87.80]	1,327	\$0.0011	$\chi^2 = 11.56, p=6.7\times 10^{-4}$
Engram	84.55%	[82.65, 86.26]	1,302	\$0.0011	$\chi^2 = 2.28, p=0.13$
BM25	80.45%	[78.40, 82.36]	1,239	\$0.0011	$\chi^2 = 17.39, p=3.0\times 10^{-5}$
Zep (published) [§] (Rasmussen et al., 2025)	~71%	—	—	—	—
Supermemory (Supermemory, 2024)	65.39%	[62.98, 67.72]	1,007	\$0.0019	$\chi^2 = 98.09, p<10^{-22}$
Mem0 (Chhikara et al., 2025)	61.43%	[58.97, 63.83]	946	\$0.0031	$\chi^2 = 6.26, p=0.012$

*EverMemOS retrieval is served by proprietary cloud infrastructure (a 4-billion-parameter GPU-hosted embedder with a Neo4j graph store); the retrieval pipeline is not open source and cannot be run on local hardware. Reported numbers use pre-computed retrieval outputs provided by the EverMemOS team.

[†]Cost per correct reflects only the harness answer and judge API calls. EverMemOS retrieval compute runs on its own proprietary infrastructure and is not included; infrastructure requirements are discussed in §5.

[‡]True Memory scores are 3-run means on the v0.6.0 pipeline. Individual run accuracies: Pro 92.79%, 93.05%, 93.05%; Base 91.75%, 92.08%, 92.21%; Edge 89.87%, 89.55%, 89.55%. Wilson CIs and correct counts are computed from the mean correct count rounded to the nearest integer.

[§]Zep accuracy is from the published Zep paper (Rasmussen et al., 2025) using their own evaluation methodology, not our harness.

2×2 contingency of paired outcomes on this subset is reported in Table 3.

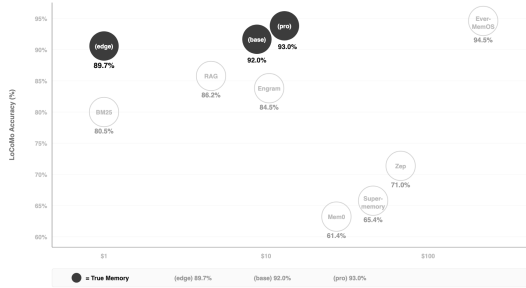
Per-category breakdown. Grouping the 357 items by LoCoMo’s four question categories and computing per-category recovery under the full-context oracle (95% Wilson CIs shown):

Category	Recov.	Count	95% CI
Cat 1 (single-sess.)	94.0%	94/100	[87.5, 97.2]
Cat 2 (multi-sess.)	87.8%	65/74	[78.5, 93.5]
Cat 3 (knowl.-upd.)	86.2%	25/29	[69.4, 94.5]
Cat 4 (temporal)	94.8%	146/154	[90.1, 97.3]

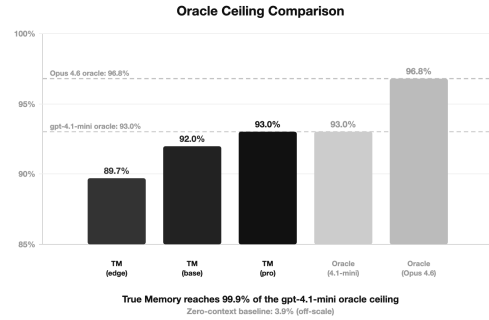
Category 3 (knowledge-update) is the smallest and the hardest-to-recover category, consistent with the intuition that contradiction-bearing questions are where a retrieval-only system is most

likely to surface stale information even when the correcting utterance is present in storage.

Residual 8% analysis. 27 of 357 questions were still answered incorrectly under full context. A best-effort qualitative pass over the wrong rows in `full_context_gpt4mini.json` places roughly 20 of the 27 in the genuine-reasoning-failure bucket (arithmetic or multi-step inference over dates, counts, or causal chains), 5 in the temporal-annotation-ambiguity bucket (questions whose gold answer fixes a calendar date that the conversation only licenses approximately), and 2 in an ambiguous/unanswerable bucket; these counts are heuristic and should be treated as provisional.



(a) **True Memory dominates the cost-accuracy Pareto frontier except for EverMemOS.** Horizontal axis: estimated monthly infrastructure cost (log scale). Vertical axis: LoCoMo accuracy.



(b) **True Memory Pro reaches 99.9% of the gpt-4.1-mini oracle ceiling.** Oracle-ceiling comparison on LoCoMo: True Memory Pro (v0.6.0, 3-run mean) reaches 99.9% of the gpt-4.1-mini ceiling and 96.0% of the Opus 4.6 ceiling.

Figure 3: Cost-accuracy and oracle-ceiling analysis on LoCoMo. (a) True Memory’s three tiers cluster at the origin of the cost axis alongside EverMemOS and other open-source systems. Paid services (Mem0, Supermemory) incur monthly costs that shift them rightward. Every non-frontier system is strictly dominated. (b) True Memory Pro consumes 256-dimensional embeddings rather than the oracle conditions’ 45.6 million input tokens per run.

Table 3: 2×2 contingency on the 357-question retrieval-bottleneck subset.

	Orac. corr.	Orac. incorr.	Total
Retr. correct	0	0	0
Retr. incorrect	330	27	357
Column total	330	27	357

Version note. The 357-question diagnostic above was run on an early pipeline iteration. On the current v0.6.0 pipeline, True Memory Pro answers 1,432 of 1,540 correctly (3-run mean), leaving approximately 108 incorrect questions. The retrieval-bottleneck hypothesis is further supported: at 93.0%, the system reaches 99.9% of the gpt-4.1-mini oracle ceiling (92.99%), so the remaining gap is dominated by questions the answer model itself cannot solve even with full context.

Horizon caveat. This diagnostic works because a full LoCoMo conversation fits in current context windows. At longer horizons of weeks, months, or years of conversation, the full history cannot be loaded into any model’s context window, so the diagnostic becomes unavailable and retrieval becomes the dominant scalable path. LoCoMo and similar benchmarks measure short-to-medium horizons, whereas True Memory’s gated ingestion, consolidation, and accumulating speaker prior are designed to scale past where these benchmarks stop

measuring.

6.3 LongMemEval (cross-benchmark generalization)

Table 4 reports systems on LongMemEval (Wu et al., 2025). True Memory Pro was evaluated on the v0.6.0 pipeline under gpt-4.1-mini; competitor rows are from a prior evaluation under the same harness conventions.

Per-category breakdown. The multi-session category is the hardest for the retrieval pipeline, consistent with LoCoMo’s per-category pattern; single-session categories score highest.

Cross-benchmark comparison. True Memory Pro leads RAG-ChromaDB on LongMemEval by 0.8 pp (87.8% vs. 87.0%) and every other agent memory product by at least 4.8 pp (EverMemOS at 83.0%). The result is consistent with the prior v0.2.0 evaluation (87.2%), indicating that the retrieval pipeline upgrades in v0.6.0 maintain cross-

Table 4: LongMemEval accuracy with 95% Wilson confidence intervals. $N = 500$. Evaluated on the LongMemEval strict variant (longmemeval_s.json). True Memory Pro is a 3-run mean on the v0.6.0 pipeline; competitor rows are single-run.

System	Accuracy	95% CI	Correct	Answer model
TM Pro (oracle variant)	92.0%	[89.43, 94.07]	460	gpt-4.1-mini
TM Pro (3-run mean, strict)	87.8%	[84.64, 90.38]	439	gpt-4.1-mini
RAG (ChromaDB)	87.0%	[83.77, 89.67]	435	gpt-4.1-mini
EverMemOS* (Hu et al., 2026)	83.0%	[79.40, 86.10]	—	gpt-4o [†]
Engram	82.2%	[78.61, 85.30]	411	gpt-4.1-mini
BM25	81.6%	[77.97, 84.75]	408	gpt-4.1-mini
Mem0 (Chhikara et al., 2025)	66.0%	[61.74, 70.02]	330	gpt-4.1-mini

*EverMemOS retrieval is served by proprietary cloud infrastructure and cannot be run on local hardware; reported number is from the EverMemOS paper.

[†]EverMemOS accuracy is from the published EverMemOS paper using gpt-4o, not our evaluation harness.

benchmark accuracy while the primary gains appear on LoCoMo and BEAM-1M.

6.4 BEAM-1M (long-horizon generalization)

BEAM (Tavakoli et al., 2026) evaluates memory at conversation scales that exceed any model’s context window. The 1M-token split contains 35 conversations with 20 questions each (700 total), spanning 10 memory-ability categories. Table 5 reports True Memory Pro (3-run mean) alongside the prior published result.

Table 5: BEAM-1M accuracy (3-run mean). $N = 700$ (35 convs \times 20 questions). Individual runs: 75.0%, 78.1%, 76.6%.

System	Acc.	Answer model
TM Pro (3-run)	76.6%	gpt-4.1-mini
Hindsight (Latimer et al., 2025)	73.9%	proprietary

Per-category breakdown. Performance varies substantially across BEAM’s ten memory-ability categories (3-run means): preference following 97.1%, contradiction resolution 91.4%, information extraction 91.4%, summarization 89.5%, instruction following 84.8%, abstention 82.4%, knowledge update 77.6%, multi-session reasoning 67.1%, temporal reasoning 64.8%, event ordering 19.5%. The top six categories exceed 80%, while event ordering (19.5%) is an outlier that requires chronological sequencing of events across sessions, a capability that the current pipeline does not specifically optimize for. Temporal reasoning

(64.8%) and multi-session reasoning (67.1%) represent the next targets for improvement.

Significance. BEAM-1M tests a qualitatively different regime from LoCoMo: at 1 million tokens per conversation, no model’s context window holds the history, and the full-context oracle diagnostic of §6.2 is unavailable. True Memory’s 76.6% exceeds the prior published Hindsight result of 73.9% by 2.7 pp, though we note that Hindsight uses a different answer model and the comparison is not controlled for that variable. The result demonstrates that the retrieval architecture generalizes from LoCoMo’s short-to-medium horizons to the long-horizon regime the system was designed for.

6.5 Abstention

Abstention is evaluated as one of the ten BEAM-1M categories (§6.4), where True Memory Pro scores 82.4% (3-run mean).

6.6 Comparison to EverMemOS

EverMemOS outscores True Memory on LoCoMo at 94.48%, 1.48 points above True Memory Pro’s 3-run mean of 93.0%. Both are retrieval-based architectures, and the gap at this margin is small. EverMemOS achieves the higher number by employing a 4-billion-parameter embedder served on GPUs, a Neo4j graph store, and a proprietary multi-service retrieval stack, whereas True Memory reaches 93.0% with a single SQLite file on commodity CPU. The 1.5-point gap separates a

GPU-served, graph-backed retrieval pipeline from one that runs on commodity CPU.

7 Ablations

This section reports a 56-configuration grid study on LoCoMo that evaluates the sensitivity of True Memory’s accuracy to component choice within the retrieval pipeline.

Grid design. We evaluated 56 combinations of 7 embedder classes \times 8 reranker options (including a no-reranker control) on LoCoMo, using the evaluation harness of §6, with hypothetical-document query expansion enabled in all 56 runs. Embedder classes spanned static 256-dimensional embeddings, dense transformer embeddings at 256, 512, 768, and 1024 dimensions, and a published retrieval-tuned dense embedding, while reranker options spanned lightweight cross-encoders, modernbert-based cross-encoders, bge-family cross-encoders, and a no-reranker control.

Aggregate results. Accuracy across the full grid ranged from 89.9% at the worst configuration to 93.1% at the best, a 3.2-percentage-point spread, with a mean of 91.26% and a median of 91.20%. Fifty-three of the 56 configurations achieved 90.0% or higher.

*Ablation data collected on the v0.4.0 pipeline. Absolute scores may differ on v0.6.0; relative rankings of embedder/reranker combinations are expected to hold (see footnote in Query Expansion Ablation below).

Subfamily behavior. Within the subfamily of a Matryoshka-trained 256-dimensional embedding (Kusupati et al., 2022) paired with any reranker, the total accuracy spread is 1.3 percentage points (best qwen3_256d \times zerank1 at 92.3%, worst qwen3.256d \times bge_large and qwen3.256d \times mxbai_large at 91.0%), so that changing the reranker identity within this family moves accuracy by at most 1.3 pp. This is the narrow-range figure referenced in the abstract.

Query expansion ablation. We additionally ran the Base configuration with and without hypothetical-document query expansion (Gao et al., 2023); enabling query expansion adds 1.0 pp on LoCoMo (92.0% without, 93.0% with, v0.6.0 3-run means).⁵

Interpretation. The grid provides a falsifiable architectural claim: if retrieval pipeline quality were primarily a matter of choosing the right embedder or reranker, we would expect wide variance across components, which is not what we observe. Within the authoritative configuration family (Matryoshka-trained 256-dimensional embedding plus any reranker), 1.3 percentage points separates the best from the worst, and within the full 56-configuration grid, 3.2 points separates the best from the worst; both ranges sit entirely above every prior published agent memory system measured in §6. What distinguishes True Memory from extraction-based competitors is not which embedder or reranker is chosen, but whether the retrieval pipeline exists as an architectural center at all.

8 Discussion

The claim this paper advances is that retrieval, rather than storage, is what determines the behavior of a memory system. The evidence is roughly 30 percentage points of LoCoMo accuracy separating True Memory from every extraction-based competitor, and roughly 19 percentage points separating its lightest configuration (Edge, 89.7%) from every extraction-based competitor. Accuracy variance across 56 component combinations within the retrieval-based regime is 3.2 percentage points, and within the top-performing subfamily it is 1.3, so that architecture separates from its absence by roughly an order of magnitude more than component choice separates from itself.

The three retrieval baselines included in §6, namely BM25 (80.5%), Engram (84.5%), and RAG-ChromaDB (86.2%), cluster within a 5.7-pp band on LoCoMo, forming a ceiling for systems that retrieve stored content without reasoning about it at query time. All three preserve events verbatim and retrieve by lexical or semantic similarity alone; none filters noise at ingestion, detects contradictions between temporally separated messages, resolves relative time references, or conditions retrieval on speaker identity. The extraction-based systems (Mem0 at 61.4%, Supermemory at

⁵Ablation data in Table 6, Table 7, and Figure 4 were collected on the v0.4.0 pipeline; absolute scores may differ on v0.6.0, but relative rankings of embedder/reranker combinations are expected to hold as these choices are independent of the gate, L0, and dedup changes introduced in v0.5.0 and v0.6.0.

Table 6: Grid-wide and subfamily statistics on LoCoMo (56 configurations, 1,540 questions).*

Scope	Cells	Best	Worst	Mean	Median	Spread
Full 56-configuration grid	56	93.1%	89.9%	91.26%	91.20%	3.2 pp
Matryoshka-256d × reranker subfamily	8	92.3%	91.0%	91.46%	91.4%	1.3 pp

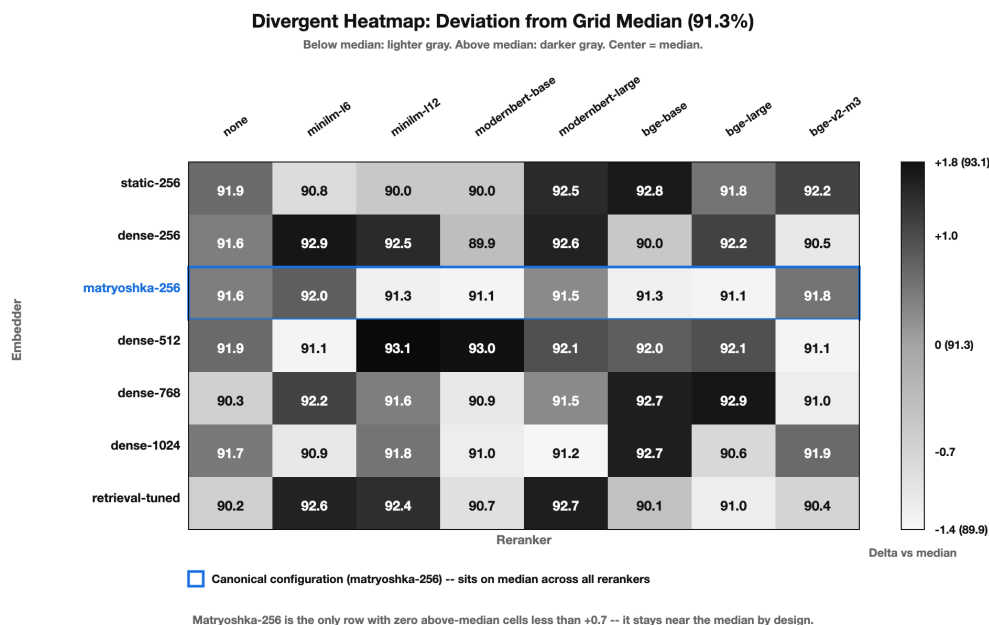


Figure 4: **The retrieval pipeline moves accuracy by at most 3.2 pp across 56 configurations; within the Matryoshka subfamily, at most 1.3 pp.*** Heatmap of the 56-configuration LoCoMo grid. Rows: 7 embedder classes. Columns: 8 reranker options including a no-reranker control. Cell color encodes accuracy from 89.9% (grid worst) to 93.1% (grid best). The Matryoshka-trained 256-dimensional embedder row shows the 1.3-percentage-point subfamily spread referenced in the abstract.

65.4%) fall roughly 20 percentage points below this ceiling because they discard the verbatim substrate entirely. True Memory Pro exceeds every baseline by 6.8 to 12.5 percentage points depending on the comparison, and even the lightweight Edge configuration exceeds RAG by 3.5 pp. The ablation of §7 shows that the gap is not attributable to any single component: within the top-performing embedder subfamily, swapping the reranker moves accuracy by at most 1.3 pp, yet every configuration in that family exceeds the best baseline by at least 4.8 pp. Three tiers of system emerge: extraction-based systems that lose information at ingestion, retrieval baselines that preserve it but surface it without query-time reasoning, and a retrieval-centered pipeline that preserves information and applies multi-stage ranking at recall. The gap between tiers is consistently wider than the gap between components within any single tier, so that the choice of retrieval architecture dominates the

choice of any individual component within it.

Two open questions define the most immediate directions for future work: the encoding gate, and horizon.

Encoding gate. The gate’s three-signal combination achieves AUC 0.816 on a held-out evaluation set (validated in a 200-variant sweep; `truememory/ingest/encoding_gate.py`), but current benchmarks inject fixed conversation transcripts and reward total recall, and therefore cannot score a system that chooses what to ingest. True Memory runs in production with selective ingestion active, and all reported results disable it for comparability; whether the gated system beats the ungated one on accuracy, and by how much, is an empirical question no public benchmark currently answers. We regard this as a gap in the evaluation literature rather than a limitation of the architecture.

Horizon. LoCoMo tests memory at scales that fit in a frontier model’s context window, which is why a full-context oracle remains computable. BEAM-1M (§6.4) begins to probe the long-horizon regime: at 1 million tokens per conversation, no model’s context window holds the history, and True Memory Pro reaches 76.6% (3-run mean). Preliminary single-run results on BEAM-10M (10 conversations at 10 million tokens each, approximately 20,000 messages per conversation, $N = 200$) reach 65.0%, an 11.6-pp drop from the 1M split. The degradation is not uniform: knowledge-update accuracy improves from 77.6% at 1M to 90.0% at 10M, suggesting that the retrieval pipeline’s contradiction-resolution mechanism benefits from deeper conversation history, while temporal reasoning (30.0%) and event ordering (5.0%) degrade sharply, consistent with the same weakness observed at 1M. A full 3-run evaluation on BEAM-10M is in progress. The agent-memory setting, however, extends to weeks, months, and years of conversation, scales at which no oracle is measurable and no benchmark yet exists. The architecture of §4 is engineered for that regime.

Verbatim event preservation yields a further architectural consequence: any scoring function introduced after ingestion can be evaluated retroactively against the full event history. A salience weighting defined later for a new domain, a retention classification, or any relevance function that did not exist at ingestion all operate on the same substrate the retrieval pipeline uses. Systems that commit to a scoring function at ingestion lack this property.

9 Conclusion

In this work we presented **True Memory**, an agent memory architecture that treats retrieval, rather than storage, as the architectural center. The system is organized as six cooperating layers over a substrate of events preserved verbatim, with an encoding gate at ingestion whose three signals (novelty, salience, prediction error) are computed through independent mechanisms, two of which query the same stored message substrate that serves retrieval.

On LoCoMo under a matched gpt-4.1-mini answer model, True Memory Pro reaches 93.0% (3-run mean), trailing only the cloud-served EverMemOS by 1.5 points while running as a sin-

gle SQLite file on commodity CPU. On Long-MemEval, the system reaches 87.8%, leading every agent memory product by at least 4.8 pp. On BEAM-1M, at 1-million-token conversation scale, True Memory Pro reaches 76.6%, above the prior published Hindsight result of 73.9%. A 56-configuration ablation shows that component choice within the retrieval pipeline moves accuracy by an order of magnitude less than the retrieval architecture itself moves it relative to extraction-based baselines, and a retrieval-bottleneck diagnostic locates the remaining errors in retrieval rather than storage.

Two directions follow. First, evaluation instruments for selective ingestion: the encoding gate (AUC 0.816, validated in a 200-variant sweep) is disabled throughout this paper because no public benchmark scores a system that chooses what to ingest, and closing this gap requires new benchmarks rather than new architectures. Second, deeper long-horizon evaluation: BEAM-1M begins to probe the regime the architecture was designed for, but weeks, months, and years of conversation remain beyond any current benchmark’s reach.

The code, evaluation harness, and benchmark outputs are available at <https://github.com/buildingjoshbetter/TrueMemory>.

Limitations

This work has three principal limitations. First, the encoding gate is disabled throughout all benchmark evaluations because no existing benchmark scores selective ingestion; the gate’s contribution to end-to-end accuracy therefore remains unmeasured. Second, the longest evaluation corpus (BEAM-1M) spans approximately one million tokens, whereas the architecture is designed for conversation histories that grow over weeks or months; no public benchmark probes this regime. Third, all reported scores use a semantic-match judge, which is more lenient than exact-match scoring; rankings across systems are valid but absolute accuracy numbers should not be compared directly to strict-match baselines without adjustment.

References

Frederic Charles Bartlett. *Remembering: A Study in Experimental and Social Psychology*. Cam-

- bridge University Press, 1932.
- Larry Cahill and James L. McGaugh. A novel demonstration of enhanced memory associated with emotional arousal. *Consciousness and Cognition*, 4(4):410–421, 1995.
- Prateek Chhikara, Dev Khant, Saket Aryan, Taranjeet Singh, and Deshraj Yadav. Mem0: Building production-ready AI agents with scalable long-term memory. *arXiv preprint arXiv:2504.19413*, 2025.
- Gordon V. Cormack, Charles L. A. Clarke, and Stefan Büttcher. Reciprocal rank fusion outperforms Condorcet and individual rank learning methods. In *Proceedings of the 32nd International ACM SIGIR Conference on Research and Development in Information Retrieval*, pages 758–759, 2009.
- Fergus I. M. Craik and Robert S. Lockhart. Levels of processing: A framework for memory research. *Journal of Verbal Learning and Verbal Behavior*, 11(6):671–684, 1972.
- Helen L. Gallagher and Christopher D. Frith. Functional imaging of “theory of mind”. *Trends in Cognitive Sciences*, 7(2):77–83, 2003.
- Luyu Gao, Xueguang Ma, Jimmy Lin, and Jamie Callan. Precise zero-shot dense retrieval without relevance labels. In *Proceedings of the 61st Annual Meeting of the Association for Computational Linguistics*, pages 1762–1777, 2023.
- Alex Garcia. sqlite-vec: A vector search SQLite extension. <https://github.com/asg017/sqlite-vec>, 2024. Accessed 2026-04-15.
- D. Richard Hipp and contributors. SQLite and the FTS5 full-text-search module. <https://www.sqlite.org/fts5.html>, 2000. SQLite released in 2000; the FTS5 module was added in 2015. Accessed 2026-04-15.
- C. Hu, X. Gao, Z. Zhou, D. Xu, Y. Bai, X. Li, H. Zhang, T. Li, C. Zhang, L. Bing, and Y. Deng. EverMemOS: A self-organizing memory operating system for structured long-horizon reasoning, 2026.
- Aditya Kusupati, Gantavya Bhatt, Aniket Rege, Matthew Wallingford, Aditya Sinha, Vivek Ramanujan, William Howard-Snyder, Kaifeng Chen, Sham Kakade, Prateek Jain, and Ali Farhadi. Matryoshka representation learning. In *Advances in Neural Information Processing Systems 35*, pages 30233–30249, 2022.
- Chris Latimer, Nicoló Boschi, Andrew Neeser, Chris Bartholomew, Gaurav Srivastava, Xuan Wang, and Naren Ramakrishnan. Hindsight is 20/20: Building agent memory that retains, recalls, and reflects. *arXiv preprint arXiv:2512.12818*, 2025.
- Patrick Lewis, Ethan Perez, Aleksandra Piktus, Fabio Petroni, Vladimir Karpukhin, Naman Goyal, Heinrich Küttler, Mike Lewis, Wen-tau Yih, Tim Rocktäschel, Sebastian Riedel, and Douwe Kiela. Retrieval-augmented generation for knowledge-intensive NLP tasks. In *Advances in Neural Information Processing Systems 33*, pages 9459–9474, 2020.
- Yuqing Li, Jiangnan Li, Mo Yu, Guoxuan Ding, Zheng Lin, Weiping Wang, and Jie Zhou. Query-focused and memory-aware reranker for long context processing. *arXiv preprint arXiv:2602.12192*, 2026.
- Adyasha Maharana, Dong-Ho Lee, Sergey Tulyakov, Mohit Bansal, Francesco Barbieri, and Yuwei Fang. Evaluating very long-term conversational memory of LLM agents. In *Proceedings of the 62nd Annual Meeting of the Association for Computational Linguistics*, pages 13851–13870, 2024. arXiv:2402.17753.
- Yu. A. Malkov and D. A. Yashunin. Efficient and robust approximate nearest neighbor search using hierarchical navigable small world graphs. *IEEE Transactions on Pattern Analysis and Machine Intelligence*, 42(4):824–836, 2018. arXiv:1603.09320.
- James L. McClelland, Bruce L. McNaughton, and Randall C. O’Reilly. Why there are complementary learning systems in the hippocampus and neocortex: Insights from the successes and failures of connectionist models of learning and memory. *Psychological Review*, 102(3):419–457, 1995.
- Rodrigo Nogueira and Kyunghyun Cho. Passage re-ranking with BERT. *arXiv preprint arXiv:1901.04085*, 2019.

- Charles Packer, Sarah Wooders, Kevin Lin, Vivian Fang, Shishir G. Patil, Ion Stoica, and Joseph E. Gonzalez. MemGPT: Towards LLMs as operating systems. *arXiv preprint arXiv:2310.08560*, 2023.
- Pinecone, Chroma, Weaviate, and Qdrant. Vector database products built on HNSW-class indexing, 2026. Representative commercial and open-source vector database products; product documentation at <https://www.pinecone.io>, <https://www.trychroma.com>, <https://weaviate.io>, and <https://qdrant.tech>, accessed 2026-04-15.
- Qwen Team. Qwen3-Embedding: Advanced text embedding and reranking through foundation models, 2025.
- Rajesh P. N. Rao and Dana H. Ballard. Predictive coding in the visual cortex: A functional interpretation of some extra-classical receptive-field effects. *Nature Neuroscience*, 2(1):79–87, 1999.
- Preston Rasmussen, Pavlo Paliychuk, Travis Beauvais, Jack Ryan, and Daniel Chalef. Zep: A temporal knowledge graph architecture for agent memory, 2025.
- Daniel L. Schacter. *The Seven Sins of Memory: How the Mind Forgets and Remembers*. Houghton Mifflin, 2001.
- Larry R. Squire and Pablo Alvarez. Retrograde amnesia and memory consolidation: A neurobiological perspective. *Current Opinion in Neurobiology*, 5(2):169–177, 1995.
- Sainbayar Sukhbaatar, Arthur Szlam, Jason Weston, and Rob Fergus. End-to-end memory networks. In *Advances in Neural Information Processing Systems 28*, pages 2440–2448, 2015. arXiv:1503.08895.
- Supermemory. Supermemory. <https://supermemory.ai/>, 2024. Commercial agent-memory service. Documentation at <https://docs.supermemory.ai>. Accessed 2026-04-15.
- Mohammad Tavakoli, Alireza Salemi, Carrie Ye, Mohamed Abdalla, Hamed Zamani, and J. Ross Mitchell. Beyond a million tokens: Benchmarking and enhancing long-term memory in LLMs. In *International Conference on Learning Representations (ICLR)*, 2026. arXiv:2510.27246.
- Stéphan Tulkens and Thomas van Dongen. Model2vec: Fast static embeddings from sentence transformers. <https://github.com/MinishLab/model2vec>, 2024. Accessed 2026-04-15.
- Endel Tulving. Episodic and semantic memory. In Endel Tulving and Wayne Donaldson, editors, *Organization of Memory*, pages 381–403. Academic Press, 1972.
- Di Wu, Hongwei Wang, Wenhao Yu, Yichong Zhang, Kai-Wei Chang, and Dong Yu. Long-MemEval: Benchmarking chat assistants on long-term interactive memory. In *International Conference on Learning Representations (ICLR)*, 2025. arXiv:2410.10813.
- Zep AI. Graphiti: A temporal knowledge graph framework for ai agents. <https://github.com/getzep/graphiti>, 2024. Accessed 2026-04-15.

A Complete 56-configuration ablation data

Table 7 lists every cell of the 7 embedder \times 8 reranker grid referenced in §7, sorted by LoCoMo accuracy. The aggregate statistics in Table 6 and the heatmap in Figure 4 are computed directly from these 56 rows.

Table 7: Per-configuration results across the 56-cell LoCoMo grid.* Wilson 95% CIs computed from correct-count over $N = 1,540$. Retrieval latency is the harness-reported average per query.

Config	Embedder	Dim	Reranker	Accuracy	Correct	95% Wilson CI	Retrieval
C01	zembed1	—	mxbai_large	93.1%	1433/1540	[91.67, 94.22]	3.29 s
C02	zembed1	—	qwen3_reranker	92.9%	1430/1540	[91.46, 94.04]	5.34 s
C03	zembed1	—	gte_reranker	92.6%	1426/1540	[91.18, 93.80]	2.69 s
C04	qwen3_256d	256	zerank1	92.3%	1421/1540	[90.83, 93.50]	3.11 s
C05	zembed1	—	bge_v2_m3	92.2%	1420/1540	[90.76, 93.44]	4.50 s
C06	nomic_768d	768	zerank1	92.0%	1417/1540	[90.55, 93.26]	2.53 s
C07	qwen3_512d	512	zerank1	92.0%	1417/1540	[90.55, 93.26]	3.06 s
C08	gte_modernbert_768d	768	gte_reranker	91.9%	1415/1540	[90.41, 93.15]	2.58 s
C09	qwen3_512d	512	qwen3_reranker	91.9%	1415/1540	[90.41, 93.15]	4.40 s
C10	zembed1	—	zerank1	91.9%	1416/1540	[90.48, 93.20]	4.08 s
C11	gte_modernbert_768d	768	bge_v2_m3	91.8%	1414/1540	[90.34, 93.09]	3.42 s
C12	qwen3_256d	256	gte_reranker	91.8%	1414/1540	[90.34, 93.09]	2.46 s
C13	gte_modernbert_768d	768	qwen3_reranker	91.7%	1412/1540	[90.20, 92.97]	4.13 s
C14	qwen3_1024d	1024	qwen3_reranker	91.7%	1412/1540	[90.20, 92.97]	4.26 s
C15	qwen3_256d	256	miniml12	91.7%	1412/1540	[90.20, 92.97]	1.92 s
C16	gte_modernbert_768d	768	zerank1	91.6%	1410/1540	[90.06, 92.85]	2.73 s
C17	qwen3_512d	512	gte_reranker	91.6%	1410/1540	[90.06, 92.85]	2.73 s
C18	zembed1	—	bge_large	91.6%	1410/1540	[90.06, 92.85]	4.42 s
C19	qwen3_512d	512	bge_v2_m3	91.5%	1409/1540	[89.99, 92.79]	3.34 s
C20	qwen3_512d	512	mxbai_large	91.5%	1409/1540	[89.99, 92.79]	2.34 s
C21	model2vec_256d	256	miniml12	91.4%	1407/1540	[89.86, 92.67]	9.41 s
C22	qwen3_256d	256	qwen3_reranker	91.4%	1407/1540	[89.86, 92.67]	4.36 s
C23	qwen3_512d	512	bge_large	91.4%	1408/1540	[89.93, 92.73]	3.34 s
C24	model2vec_256d	256	bge_large	91.3%	1406/1540	[89.79, 92.61]	3.39 s
C25	nomic_768d	768	qwen3_reranker	91.3%	1406/1540	[89.79, 92.61]	4.01 s
C26	qwen3_256d	256	bge_v2_m3	91.3%	1406/1540	[89.79, 92.61]	3.50 s
C27	qwen3_512d	512	miniml12	91.3%	1406/1540	[89.79, 92.61]	2.11 s
C28	gte_modernbert_768d	768	bge_large	91.2%	1405/1540	[89.72, 92.55]	3.14 s
C29	gte_modernbert_768d	768	miniml12	91.2%	1404/1540	[89.65, 92.49]	1.86 s
C30	gte_modernbert_768d	768	no_reranker	91.2%	1404/1540	[89.65, 92.49]	1.71 s
C31	nomic_768d	768	bge_large	91.2%	1404/1540	[89.65, 92.49]	3.56 s
C32	qwen3_256d	256	no_reranker	91.2%	1404/1540	[89.65, 92.49]	1.81 s
C33	gte_modernbert_768d	768	mxbai_large	91.1%	1403/1540	[89.58, 92.43]	2.63 s
C34	qwen3_512d	512	no_reranker	91.1%	1403/1540	[89.58, 92.43]	1.89 s
C35	model2vec_256d	256	zerank1	91.0%	1402/1540	[89.51, 92.37]	3.78 s
C36	nomic_768d	768	no_reranker	91.0%	1402/1540	[89.51, 92.37]	1.74 s
C37	qwen3_256d	256	bge_large	91.0%	1401/1540	[89.44, 92.31]	3.48 s
C38	qwen3_256d	256	mxbai_large	91.0%	1401/1540	[89.44, 92.31]	2.30 s
C39	nomic_768d	768	bge_v2_m3	90.9%	1400/1540	[89.37, 92.24]	3.04 s
C40	nomic_768d	768	miniml12	90.9%	1400/1540	[89.37, 92.24]	1.92 s
C41	qwen3_1024d	1024	bge_v2_m3	90.9%	1400/1540	[89.37, 92.24]	3.63 s
C42	qwen3_1024d	1024	miniml12	90.9%	1400/1540	[89.37, 92.24]	2.09 s
C43	nomic_768d	768	mxbai_large	90.8%	1398/1540	[89.23, 92.12]	2.34 s
C44	qwen3_1024d	1024	no_reranker	90.8%	1399/1540	[89.30, 92.18]	1.86 s
C45	qwen3_1024d	1024	zerank1	90.8%	1399/1540	[89.30, 92.18]	3.62 s
C46	qwen3_1024d	1024	gte_reranker	90.7%	1397/1540	[89.16, 92.06]	2.62 s
C47	qwen3_1024d	1024	mxbai_large	90.7%	1397/1540	[89.16, 92.06]	2.25 s
C48	model2vec_256d	256	gte_reranker	90.6%	1395/1540	[89.02, 91.94]	2.36 s
C49	zembed1	—	miniml12	90.6%	1395/1540	[89.02, 91.94]	26.86 s
C50	model2vec_256d	256	qwen3_reranker	90.5%	1394/1540	[88.95, 91.88]	4.21 s
C51	zembed1	—	no_reranker	90.5%	1393/1540	[88.88, 91.82]	1.54 s
C52	nomic_768d	768	gte_reranker	90.4%	1392/1540	[88.82, 91.76]	2.54 s
C53	qwen3_1024d	1024	bge_large	90.1%	1387/1540	[88.47, 91.46]	3.38 s
C54	model2vec_256d	256	bge_v2_m3	89.9%	1385/1540	[88.33, 91.34]	3.41 s
C55	model2vec_256d	256	mxbai_large	89.9%	1384/1540	[88.26, 91.28]	2.25 s
C56	model2vec_256d	256	no_reranker	89.9%	1384/1540	[88.26, 91.28]	1.61 s